Title

Spontaneous Single-Copy Loss of TP53 in Human Embryonic Stem Cells Markedly Increases Cell Proliferation and Survival

Journal

Stem Cells, 35(4)

ISSN

1066-5099

Authors

Amir, Hadar
Touboul, Thomas
Sabatini, Karen
et al.

Publication Date

2017-04-01

DOI

10.1002/stem.2550

Peer reviewed

PHCbi

70% of surveyed scientists admitted that they could not replicate someone else's research.[1]

50% admitted that they couldn't replicate their own research.[1]

Stem Cells Demand Reproducibility.

PHCbi brand Cell-IQ™ CO_2 and O_2 incubators are designed to deliver reproducibility critical to stem cell research and regenerative medicine.

Your desired temperature and gas concentrations replicate the *in vivo* model of any cell culture environment with precision and predictability. Our SafeCell™ and inCu-saFe® technologies protect your work *in vitro*. Learn more at **www.phchd.com/us/biomedical/cell-culture-incubators.**

Select from eight models including your choice of high heat or H_2O_2 decontamination with CO_2 or CO_2/O_2 control.

PHC Corporation of North America

PHC Corporation of North America
1300 Michael Drive, Suite A, Wood Dale, IL 60191
Toll Free USA (800) 858-8442, Fax (630) 238-0074
www.phchd.com/us/biomedical

1) Baker, Monya. "1,500 scientists lift the lid on reproducibility." Nature, no. 533 (May 26, 2016): 452-54. doi:10.1038/533452a.

PHC Corporation of North America is a subsidiary of PHC Holdings Corporation, Tokyo, Japan, a global leader in development, design and manufacturing of laboratory equipment for biopharmaceutical, life sciences, academic, healthcare and government markets.

STEM CELLS®

EMBRYONIC STEM CELLS/INDUCED PLURIPOTENT STEM CELLS

Spontaneous Single-Copy Loss of *TP53* in Human Embryonic Stem Cells Markedly Increases Cell Proliferation and Survival

HADAR AMIR,[a] THOMAS TOUBOUL,[a] KAREN SABATINI,[a] DIVYA CHHABRA,[a] IBON GARITAONANDIA,[b] JEANNE F. LORING,[b] ROBERT MOREY,[a] LOUISE C. LAURENT[a]

Key Words. Embryonic stem cells • Chromosomal aberrations • p53 • Proliferation • DNA repair

[a]Department of Reproductive Medicine, University of California, San Diego, La Jolla, California, USA; [b]Center for Regenerative Medicine, Department of Chemical Physiology, The Scripps Research Institute, La Jolla, California, USA

Correspondence: Louise C. Laurent, M.D., Ph.D., Department of Reproductive Medicine, Division of Maternal Fetal Medicine, The Sanford Consortium for Regenerative Medicine, University of California, San Diego, 2880 Torrey Pines Scenic 9500 Gilman Drive, MC0695, La Jolla, California 92093-0695, USA. Telephone: 858-246-1403; Fax: 858-534-8329; e-mail: llaurent@ucsd.edu

Received January 18, 2016; accepted for publication November 1, 2016; first published online in STEM CELLS *EXPRESS* November 26, 2016.

1066-5099/2016/$30.00/0

http://dx.doi.org/10.1002/stem.2550

ABSTRACT

Genomic aberrations have been identified in many human pluripotent stem cell (hPSC) cultures. Commonly observed duplications in portions of chromosomes 12p and 17q have been associated with increases in genetic instability and resistance to apoptosis, respectively. However, the phenotypic consequences related to sporadic mutations have not been evaluated to date. Here, we report on the effects of a single-copy deletion of the chr17p13.1 region, a sporadic mutation that spontaneously arose independently in several subclones of a human embryonic stem cell culture. Compared to cells with two normal copies of chr17p13.1 ("wild-type"), the cells with a single-copy deletion of this region ("mutant") displayed a selective advantage when exposed to stressful conditions, and retained a higher percentage of cells expressing the pluripotency marker POU5F1/OCT4 after 2 weeks of in vitro differentiation. Knockdown of *TP53*, which is a gene encompassed by the deleted region, in wild-type cells mimicked the chr17p13.1 deletion phenotype. Thus, sporadic mutations in hPSCs can have phenotypic effects that may impact their utility for clinical applications. STEM CELLS *2017;35:872–885*

SIGNIFICANCE STATEMENT

hPSCs acquire sporadic mutations in culture, which can potentially affect their phenotypic characteristics. We explored whether a sporadic mutation that spontaneously arose in a human embryonic stem cell culture consisting of a single-copy deletion of chr17p13.1 would confer a survival advantage to the mutant cells. We found that the mutant cells displayed a selective advantage when exposed to stressful conditions compared to the wild-type cells. Knockdown of TP53, which is a gene encompassed by the deleted region, in wild-type cells mimicked the chr17p13.1 deletion phenotype. Thus, phenotypic implications of sporadic mutations must be taken into consideration before using hPSCs for clinical applications.

INTRODUCTION

It has been observed that genomic abnormalities arise in human embryonic stem cell (hESC) lines during prolonged in vitro culture [1–3], and are more common in cultures that have been enzymatically passaged [4, 5] or propagated in feeder-free conditions [5, 6]. Duplications of portions of chromosomes 12 (particularly 12p) [3, 7, 8], 17 (usually 17q) [8], 20 (particularly 20q) [3, 9–11], and X [3, 7] have been seen in multiple hESC lines. The chromosome 12 and 17 duplications are commonly found in germ cell tumors [12, 13], and all of these duplicated regions include genes associated with cell growth and/or survival. The chromosome 12 duplication has been linked to increased genetic instability [14], and a common duplication of chr20q11.21 has been shown to confer resistance to apoptosis [15, 16]. Taken together, these reports suggest that common genetic aberrations seen in multiple independent hESC lines can confer selective advantages to the cells carrying them. However, the potential phenotypic consequences of sporadic aberrations that are observed only in single hESC lines have not yet been studied.

In a study comparing the genetic stability of hESCs and human induced pluripotent stem cells (hiPSCs) cultured in different conditions, we identified a region of the short arm of chromosome 17 that underwent single-copy, hemizygous, deletion in several subcultures of WA09 hESCs [5]. In the different subcultures, the boundaries of the deleted region varied, but there was a small (154.5 kb) overlap region. As will be discussed below, this region encompasses

the key tumor suppressor gene *TP53*. In somatic cells, TP53 is the "guardian of the genome," linking stress signals to downstream processes, including apoptosis, cell cycle arrest, DNA repair and senescence [17]. TP53 function is frequently compromised during tumorigenesis as a result of homozygous somatic mutations, which are seen in more than 50% of human cancers [18]. Single-copy deletion of chr17p13.1, the genomic region containing *TP53*, has been strongly associated with chemotherapy failure and poor prognosis in multiple cancers [19–22]. *TP53* has been implicated as the driver mutation for these clinical outcomes, and studies have suggested that monoallelic inactivation of *TP53* is sufficient for poor prognosis, including resistance to treatment (particularly for agents whose effects are mediated by the TP53 pathway) and clonal selection [19–25].

In hESCs, TP53 appears to maintain a balance between proliferation, self-renewal, and differentiation [26]. hESCs express high levels of TP53 mRNA and protein, which subsequently decrease during differentiation [27]. Exposing hESCs to DNA damaging agents leads to increased accumulation of TP53 [28, 29], translocation of TP53 to the nucleus [29, 30], apoptosis [28, 30], decreased mRNA and protein expression of POU5F1/OCT4 and NANOG [28], and spontaneous differentiation [28]. *TP53* knockdown reduces DNA damage-induced and spontaneous apoptosis and differentiation, and promotes survival and expansion of hESCs [28, 30].

In this study, we characterized the phenotype of hESCs carrying a single-copy deletion of chr17p13.1 that spontaneously arose during culture, and identified *TP53* as a gene that contributes significantly to the phenotype conferred by this mutation.

Materials and Methods

Generation and Culture of Wild-Type and Mutant WA09 hESC Clones

Single-cell clones were generated from the original mosaic MefEnz p104_D culture by manually picking single cells and placing them on mouse embryo fibroblast (MEF) feeder layers. The resulting clones were cultured on either MEF feeder layers in standard hPSC medium or on Geltrex (Thermo Fisher Scientific, Waltham, MA, www.thermofisher.com) in mouse embryo fibroblast conditioned medium (MEF-CM) with 12 ng/ml basic FGF (bFGF) or in E8 medium (Thermo Fisher Scientific, Waltham, MA, www.thermofisher.com). All cultures were tested for mycoplasma monthly. Please see Supporting Information Experimental Procedures for details.

Short Hairpin RNA (shRNA) Knockdown of *TP53*

The wild-type hESC clones were transduced with three lentiviral vectors containing shRNAs against the TP53 mRNA and one negative control shRNA vector (four vectors total), and selected with puromycin. Please see Supporting Information Experimental Procedures for details.

Phenotypic Characterization of hESC Clones

Cell proliferation, apoptosis, and cell cycle distribution were assessed using the 3-(4,5-dimethylthiazol-2-yl)-2,5-diphenyltetrazolium bromide (MTT) Kit (Roche, Basel, Switzerland, www.roche.com), Annexin V Apoptosis Detection Kit I (BD Biosciences), and the Click-iT 5-ethynyl-2'-deoxyuridine (EdU) Alexa Fluor 647 Flow Cytometry Kit (Thermo Fisher Scientific, Waltham, MA, www.thermofisher.com), respectively, according to the manufacturers' protocols. Clonogenicity was evaluated by seeding the cells at low density and staining the colonies at 7 days with alkaline phosphatase. Expression of pluripotency and differentiation markers was assessed by immunocytochemistry. Differentiation potential was evaluated by embryoid body (EB; in vitro) and teratoma (in vivo) formation, and immunocytochemistry. Expression of specific proteins was assessed by western blot. Please see Supporting Information Experimental Procedures for details.

Molecular Analysis of hESC Clones

DNA and RNA extraction were performed using the DNeasy Blood and Tissue Genomic DNA Purification Kit (Qiagen, Hilden, Germany, www.qiagen.com) and the Nucleo Spin RNAII kit (Takara Bio USA, Inc., Mountain View, CA, www.clontech.com) for quantitative real-time-polymerase chain reaction (qRT-PCR), and the mirVana miRNA Isolation Kit (Life Technologies, Inc.) for RNA-Seq, respectively, following the manufacturers' instructions. Copy number variant (CNV) values were determined using TaqMan Copy Number Assays (Thermo Fisher Scientific, Waltham, MA, www.thermofisher.com) and the HumanOmni5-4 BeadChip (Illumina, Inc., San Diego, CA, www.illumina.com) using CNVPartition 3.2.0 as the CNV-calling algorithm. RNA-Seq libraries were generated using the Illumina TruSeq Stranded mRNA Sample Prep Kit (Illumina, Inc., San Diego, CA, www.illumina.com) and sequenced on a HiSeq 2500 (Illumina, Inc., San Diego, CA, www.illumina.com). Please see Supporting Information Experimental Procedures for details.

Comet Assay

The Comet assay was performed using the OxiSelect Comety assay kit (Cell Biolabs, Inc., San Diego, CA, www.cellbiolabs.com) according to the manufacturer's protocol. Briefly, 100,000 cells were seeded per well in Essential 8 medium. To induce DNA damage, the cells were treated for 24 hours with 1 μm Etoposide. Control cells were not treated. Please see Supporting Information Experimental Procedures for details.

Data Analysis

Details of data analysis procedures are described in the Supporting Information Experimental Procedures. Briefly, for phenotypic characterization and qRT-PCR experiments, data were obtained from 2 to 3 independent biological experiments, with each experiment including at least three replicates, and comparisons were performed using Student's *t* test. For the Single nucleotide polymorphism (SNP) Genotyping experiment, data analysis was performed using GenomeStudio (Illumina, Inc., San Diego, CA, www.illumina.com), with the CNVPartition Plug-in. RNA-Seq data were analyzed using a variety of data cleaning, mapping, and analysis tools.

Results

Establishment of Clonal WA09 hESC Sublines with and Without a Deletion in Chr17p13.1

Previously, we identified copy number (CN) aberrations that arose in hESCs and hiPSCs over long-term culture in different

conditions, with the most frequent aberrations being duplications of chr20q11.21 and chr12p13.31, and deletions of chr17p13.1 [5]. The chr20 and chr12 duplications have been observed in several studies in many different hPSC lines. However, the chr17p13.1 deletion, which encompasses the *TP53* gene, had not been described before in the human embryonic stem cell literature, and therefore was of interest to us. Among multiple WA09 hESC subcultures with overlapping single-copy deletions of portions of chromosome 17 [5], which varied in size from 158,481 to 16,272,121 bases, we selected the subculture (MefEnz p104_D) that carried both one of the smallest deletions in the chr17p13.1 region, and the fewest other detected aberrations for further study. Targeted copy-number analysis by qRT-PCR was used to validate the chr17p13.1 deletion. Results for the MefEnz p104_D subculture showed that the cell population carried an average of 1.43 copies of this region (Fig. 1A; Supporting Information Table S1), indicating that the population was mosaic for this aberration. To obtain pure populations of WA09 hESCs with and without the chr17p13.1 deletion, we used single-cell cloning to isolate clones carrying one copy (clones 2 and 17, the "mutant" clones) or two copies (clones 3 and 6, the "wild-type" clones) of the chr17p13.1 region, as determined by CNV-qRT-PCR (Fig. 1B; Supporting Information Table S1).

Since the MefEnz p104_D subculture also showed CN aberrations at four other genomic locations in our previous study [5], we performed genome-wide SNP genotyping using the HumanOmni5-4 BeadChip Array to evaluate these loci in each of the four clones (Supporting Information Fig. S1; Supporting Information Table S2). The chr12p13.31 duplication was calculated to be a 3-copy duplication in all four clones using the automated CNV detection software, but on inspection of the B Allele Frequency (BAF) plots, this aberration was consistent with a higher CN duplication. In either case, the number of copies appeared to be the same in all four clones. In contrast, the wild-type and mutant clones showed differences in CN for the other four previously identified genomic aberrations. Only the mutant clones carried the deletion of chr17p13.1 and the duplications of chr17q23.1 and the X chromosome. The only gene contained within the chr17q23.1 region was PTRH2, which has been associated with cancer and apoptosis [31–33], but whose role in tumorigenesis is not well understood. Both duplications and deletions of the X chromosome are frequently observed in human tumors, but are also correlated with increasing age [34, 35], leading some to conclude that X chromosome numerical aberrations were likely to be a secondary event, and not important in the pathogenesis of cancers [35]. Finally, the SNP genotyping data showed that the chr20q11.21 duplication was present in all four clones, but suggested that the number of copies was higher in the wild type compared to the mutant clones.

SNP genotyping analysis of the four clones also revealed seven CN aberrations that were not detected in the MefEnz p104_D subculture in our previous study [5]: four duplications that were common among the four clones, and three deletions that were unique to the two wild-type clones. We postulate that these aberrations were not identified previously because a lower-resolution SNP genotyping microarray (the Human Omni1-4) was used in the prior study.

Since the BAF plots indicated that the chr12p13.1 and chr20q11.21 regions appeared to have higher CN duplications, we further evaluated them with CNV-qRT-PCR using probes in the *NANOG* and *BCL2L1* genes, which are located within these two genomic regions. For the chr12p13.31 duplication, the CNV-qRT-PCR results were consistent with four to five copies in all four clones (Fig. 1C; Supporting Information Table S1). Estimates of the exact number of copies by CNV-qRT-PCR become less accurate as the number of copies increases [36], and it is not possible to reliably distinguish between four or five copies. Since both the wild-type and the mutant clones had similar numbers of copies, we reasoned that the chr12p13.31 duplication should not cause differential effects in the wild-type and mutant clones.

For the chr20q11.21 region, the CNV-qRT-PCR results were consistent with five copies of the *BCL2L1* gene in both of the wild-type clones, and three copies in both of the mutant clones (Fig. 1C; Supporting Information Table S1). To correlate CN with protein expression, we performed western blot analysis. *BCL2L1* can produce two isoforms by alternative splicing: an anti-apoptotic isoform, Bcl-X_L, and a pro-apoptotic isoform, Bcl-X_S. There was significantly higher expression of Bcl-X_L protein in the wild type compared to mutant clones (two-fold difference, $p < .005$), but no significant difference in Bcl-X_S protein expression (Fig. 1D, 1E; Supporting Information Table S1), resulting in a significant difference in the Bcl-X_L:Bcl-X_S ratio between the mutant and wild-type cells ($p = .033$) (Fig. 1F; Supporting Information Table S1). Since the Bcl-X_L:Bcl-X_S ratio influences the sensitivity of hESCs to apoptotic stimuli [15, 16], the higher CN of the chr20q11.21 region and higher Bcl-X_L:Bcl-X_S ratio in the wild-type cells should confer a survival advantage to the wild-type cells over the mutant cells. This result implies that if the mutant cells display an overall survival advantage over the wild-type cells, then the mutant cells carry a genetic (or epigenetic) change that has a stronger effect than the difference in the number of copies of the chr20q11.21 region.

Considering these results, together with what is known in the literature about the genes contained within each of the observed CN aberrations, we deemed that it was likely that at least some of the phenotypic differences displayed by the mutant clones would be attributable to the single-copy deletion of chr17p13.1, and therefore focused on this region for further study.

Use of Transcriptomic Profiling to Identify Likely Phenotypic Effects of Single-Copy Deletion of Chr17p13.1

The chr17p13.1 region affected by the deletion contains 17 genes, including *TP53*. To enable us to focus on the most likely phenotypic effects of this deletion, we compared the transcriptomes of the mutant and wild-type clones, and performed functional enrichment analysis on the differentially expressed genes. We performed RNAseq on the four clones cultured in E8 medium (three biological replicates per clone). Unsupervised hierarchical clustering demonstrated clear separation of the 12 samples according to genetic status (mutant vs. wild-type) (Supporting Information Fig. S2A). We then identified transcripts that were differentially expressed between the mutant and wild-type clones (Supporting Information Table S3, adjusted p value $< .05$ and absolute log2 fold-change > 1.2), and performed functional enrichment analysis to identify regulatory pathways that were highly

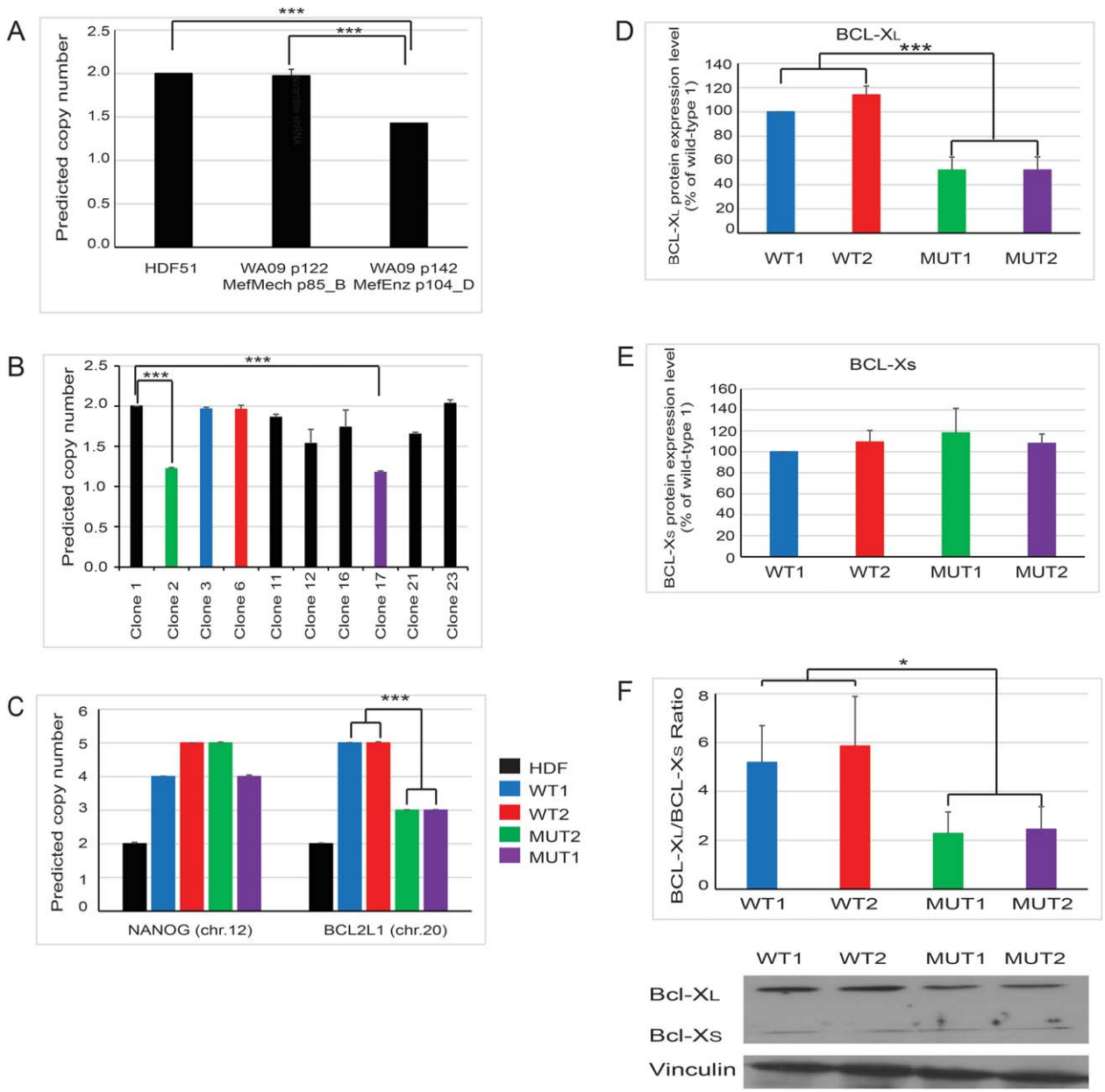

Figure 1. Generation of pure subpopulations of WA09 hESCs that are wild-type or mutant for the single-copy deletion of Chr17p13.1. **(A)**: chr17p13.1 copy number (CN) in the WA09 MefMech p85_B and WA09 MefEnz p104_D sub-cultures (+/− deletion [5], respectively) was measured using a CNV-qRT-PCR assay for the *TP53* gene (Hs00347385_cn assay [Life Technologies]). A CN value of 2 indicates the presence of two alleles (i.e., normal); a CN of 1 indicates a single-copy deletion. HDF51 fibroblast cells were used as a normal reference. **(B)**: The CN of 10 clones obtained by single cell cloning from the WA09 MefEnz p104_D subculture, using CNV-qRT-PCR for the *TP53* gene, with clone 1 cells as reference. The clones chosen for this study are highlighted in the colored bars. **(C)**: The CN for the chr12p13.31 and the chr20q11.21 regions were measured by CNV-qRT-PCR for the *NANOG* (Hs03838104_cn) and *BCL2L1* (Hs07186557_cn*)* mRNAs, respectively, with HDF51 cells as reference. See also Supporting Information Figure S1 and Supporting Information Table S1. **(D)**: Quantification of Bcl-X_L protein levels, using wild-type 1 as reference. **(E)**: Quantification of Bcl-X_S protein levels, using wild-type 1 as reference. **(F)**: Ratio between the protein levels of the Bcl-X_L and Bcl-X_S isoforms, using wild-type 1 as reference. A representative image of the western blot is shown below the graph. Vinculin was used as a loading control. CNV-qRT-PCR assays: mean ± standard error of the mean (SEM) of technical triplicates. Western blots: mean ± SEM of three biological replicates. Two-tailed *t* test; $*p < .05$, $**p < .01$, $***p < .005$. Abbreviations: MUT, mutant; WT, wild type.

represented in the differentially expressed lists of transcripts (DAVID, adjusted p value $< .001$ for GO Biological Processes [GO BPs] and $< .05$ for KEGG Pathways[48]). Transcripts that were more highly expressed in the mutant compared to the wild-type clones were analyzed separately from those that were more highly expressed in the wild-type than the mutant clones. Transcripts that were more highly expressed in the mutant clones were not significantly enriched for any GO BPs or KEGG Pathways, while those that were more highly expressed in the wild-type clones were enriched for many categories (Table 1). Inspection of the enriched GO BPs and KEGG Pathways revealed that the enriched categories could be classified into four general groups, which we have labeled with the most significantly enriched category for each group:

Table 1. Gene ontology and KEGG pathways enriched in the set of genes differentially expressed between wild-type and mutant clones

	chr17p13.1 deletion > WT		WT > chr17p13.1 deletion	
GO Biological Process enrichment	GO BP category	B-H	GO BP category	B-H
	None with B-H <0.001	NA	GO:0048598~embryonic morphogenesis	7.34E-10
			GO:0007369~gastrulation	7.37E-07
			GO:0007389~pattern specification process	1.39E-06
			GO:0001704~formation of primary germ layer	9.78E-06
			GO:0022610~biological adhesion	4.96E-05
			GO:0003002~regionalization	4.96E-05
			GO:0007155~cell adhesion	5.54E-05
			GO:0001501~skeletal system development	5.69E-05
			GO:0042127~regulation of cell proliferation	1.63E-04
			GO:0009952~anterior/posterior pattern formation	2.85E-04
			GO:0009792~embryonic development ending in birth or egg hatching	2.98E-04
			GO:0007156~homophilic cell adhesion	4.15E-04
			GO:0060485~mesenchyme development	4.66E-04
			GO:0048762~mesenchymal cell differentiation	4.68E-04
			GO:0014031~mesenchymal cell development	4.68E-04
			GO:0035295~tube development	4.80E-04
			GO:0043009~chordate embryonic development	5.06E-04
			GO:0016337~cell-cell adhesion	7.80E-04
			GO:0001707~mesoderm formation	8.24E-04
			GO:0001667~ameboidal cell migration	9.42E-04
KEGG Pathway enrichment	KEGG Pathway category	B-H	KEGG Pathway category	B-H
	None with B-H <0.05	NA	hsa04310:Wnt signaling pathway	0.009
			hsa04060:Cytokine-cytokine receptor interaction	0.012
			hsa04115:p53 signaling pathway	0.052
			hsa05217:Basal cell carcinoma	0.039
			hsa05218:Melanoma	0.043
			hsa04080:Neuroactive ligand-receptor interaction	0.047

CER1	LHX1
CHRD	MESP1
CRABP2	MIXL1
DKK1	MSX1
DLC1	MSX2
EOMES	NKX3-2
EYA1	NODAL
FGF10	ODZ4
FGF4	PROX1
FGF8	PRRX1
FOXA2	RET
FOXC1	ROR2
GAS1	SLIT2
GATA4	SP8
GBX2	T
GJA5	TBX6
GSC	TWIST1
HES1	WNT3
HOXA1	WNT3A
HOXB1	ZEB1
ITGA8	ZEB2
LEF1	

embryonic morphogenesis
biological adhesion
regulation of cell proliferation
p53 signaling pathway

embryonic morphogenesis; biological adhesion; regulation of cell proliferation; and p53 (TP53) signaling pathway. Of course, enrichment for genes in the TP53 signaling pathway would be expected given the known difference in CN of the *TP53* gene between the mutant and wild-type clones. In order to identify the specific phenotypes downstream of TP53, mostly likely to be perturbed in the mutant clones, we mapped the elements in the TP53 pathway that were differentially expressed in the mutant and wild-type clones, including the direction of differential expression (Table 1; Supporting Information Fig. S2B–S2D). With the exception of two factors, IGF-BP3 and GADD45G, which had markedly lower expression levels and higher (less significant) *p* values than the other differentially expressed members of the pathway, we found that all of the members of the TP53 pathway showed differential expression in the direction that was consistent with a decrease in TP53 activity in the mutant clones. Further, these changes in expression of genes in the TP53 pathway predicted increases in cell cycle progression and angiogenesis/metastasis and decreases in apoptosis and DNA repair (Supporting Information Fig. S2B). From these analyses, we judged that we would be most likely to observe differences in cell proliferation, cell adhesion and dependence on cell adhesion, apoptosis, DNA repair, and differentiation, and undertook experiments to evaluate these phenotypes in the mutant and wild-type clones.

Effect of Single-Copy Deletion of Chr17p13.1 on Cell Proliferation of hESCs

We examined the proliferation rate of the wild-type and mutant clones in two feeder-free culture conditions, one in MEF-CM, which is a complex, undefined medium considered to be the richest feeder-free culture condition, and the other in E8 medium, which in contrast is a completely defined "minimal" hESC medium.

Each clone was seeded at four cell concentrations, and a MTT assay was performed daily for four consecutive days. All four clones proliferated well in both conditions at all four plating concentrations (Fig. 2A, 2B, Supporting Information Fig. S3A–S3H; Supporting Information Table S1), with higher proliferation in MEF-CM than E8, particularly for the lower initial cell concentrations. No significant differences were observed between the proliferation rates of the wild-type and mutant clones in MEF-CM (Fig. 2A, Supporting Information Fig. S3A–S3D; Supporting Information Table S1), but in E8, the proliferation rates of the mutant clones were consistently and significantly higher than those of the wild-type clones starting on day 3 for all but the highest plating concentration (Fig. 2B, Supporting Information Fig. S3E–S3H; Supporting Information Table S1). These results suggest that the chr17p13.1 deletion permits the hESCs to proliferate at a higher rate in more restrictive growth conditions.

To determine whether the increased cell proliferation in the mutant clones was the result of a difference in cell cycle regulation, we evaluated the cell cycle distribution of wild-type and mutant cells in E8 medium using EdU incorporation and quantitative DNA staining with VxCycle Violet, followed by analytical fluorescence activated cell sorting (FACS). Our results revealed a significantly higher fraction of cells in S phase and lower fraction in G1/G0 in the mutant compared with the wild-type clones (Fig. 2E, Supporting Information Fig. S3I–S3M; Supporting Information Table S1). Collectively, these results suggest that a single-copy deletion of chr17p13.1 was associated with enhanced proliferation by promoting G1-to-S cell cycle progression in the mutant hESCs.

Effect of Single-Copy Deletion of Chr17p13.1 on Clonogenicity of hESCs

Single-cell dissociation of hPSCs and many other cell types rapidly induces apoptosis, resulting in poor clonogenicity [37].

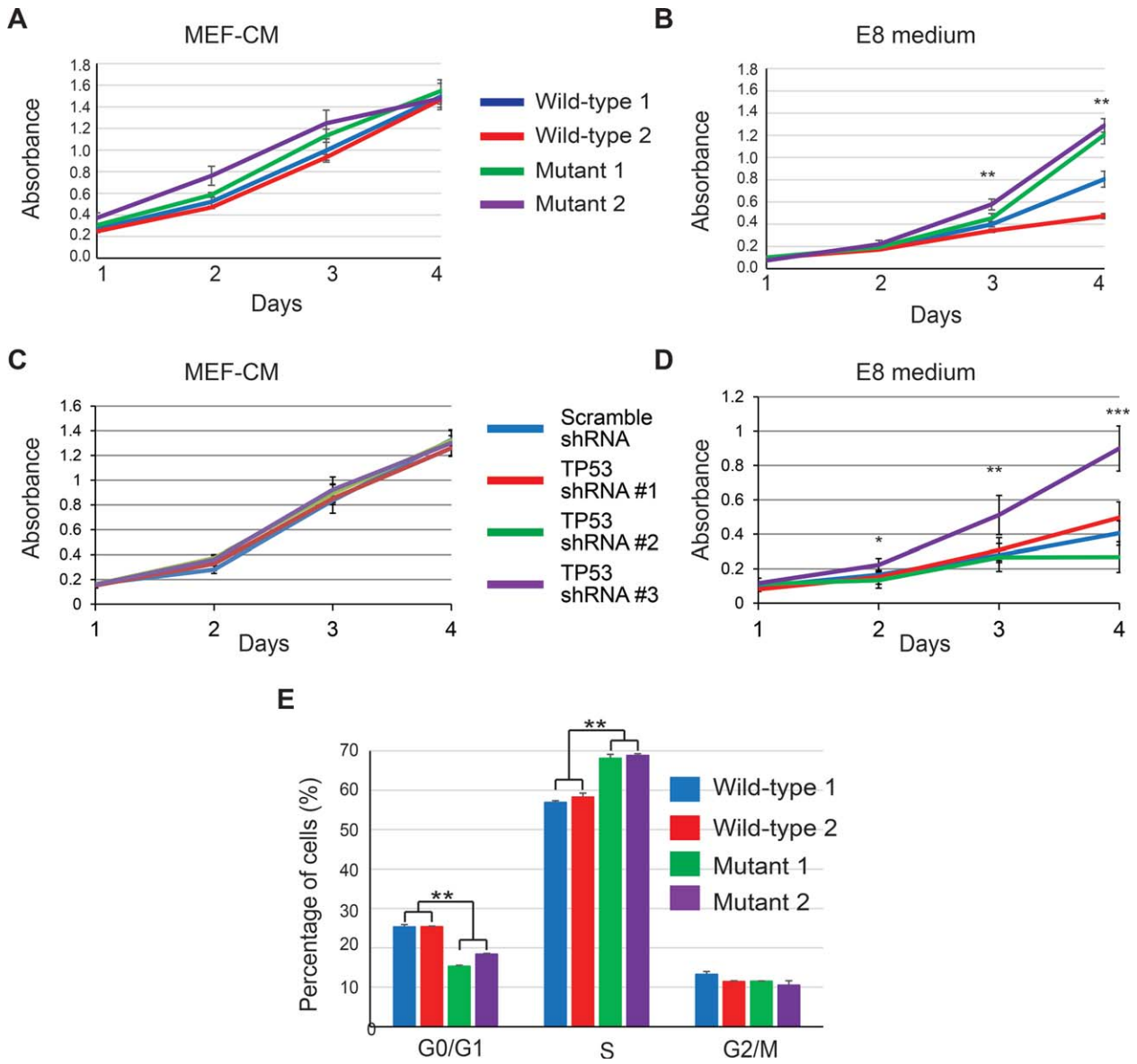

Figure 2. Cell proliferation rate and cell cycle distribution for wild-type and mutant, and TP53 shRNA knockdown, hESC clones. **(A–D)**: The proliferation of the wild-type and the mutant clones (A, B) and TP53 shRNA knockdown clones made in wild-type clone 1 (C, D) cultured in MEF-CM (A, C) and E8 medium (B, D) was determined by MTT assay. Representative data for cells plated at a density of 5,000 cells per well in 96 well plates are shown. *p value $<$ .01, **p value $<$ .005, ***p value $<$ .0001. See also Supporting Information Figure S2A–S2H. **(E)**: Histogram showing a comparison between the cell-cycle distributions of the wild-type and mutant clones. **p value $<$ .005. See also Supporting Information Figure S3A. Abbreviation: MEF-CM, mouse embryo fibroblast conditioned medium.

In contrast, a well-known characteristic of malignant cells is the ability to escape dissociation-induced apoptosis, and this phenomenon is strongly associated with mutations in *TP53* [38]. We investigated the effect of single-copy deletion of chr17p13.1 on the clonogenic capacity of hESCs by plating 100 single cells per well in six-well culture plates containing MEF feeder layers. After 7 days, hESC colonies were stained for alkaline phosphatase activity and counted. The clonogenic efficiency was determined by averaging the number of colonies obtained in three independent experiments, with each experiment including triplicate wells for each clone. The results showed that the clonogenic potential of the mutant hESCs was approximately twice as high as that of their wild-type counterparts (average of 29%–33% for the wild-type vs. 56%–62% for the mutant clones, $p < .005$) (Fig. 3A, Supporting Information Fig. S4A; Supporting Information Table S1).

Effect of Single-Copy Deletion of Chr17p13.1 on Staurosporine-Induced Apoptosis of hESCs

Staurosporine induces apoptosis in many cell types via the activation of both TP53-dependent and TP53-independent pathways, but far more efficiently through the first mechanism. Annexin V/PI staining and flow cytometry were used to analyze the rate of early apoptotic, late apoptotic, and necrotic cells with and without staurosporine treatment. The fractions of early and late apoptotic cells were significantly higher for wild-type clones treated with 0.1 μM staurosporine for 20 hours compared with the mutant clones ($p = .006$ and $p < .005$, for early

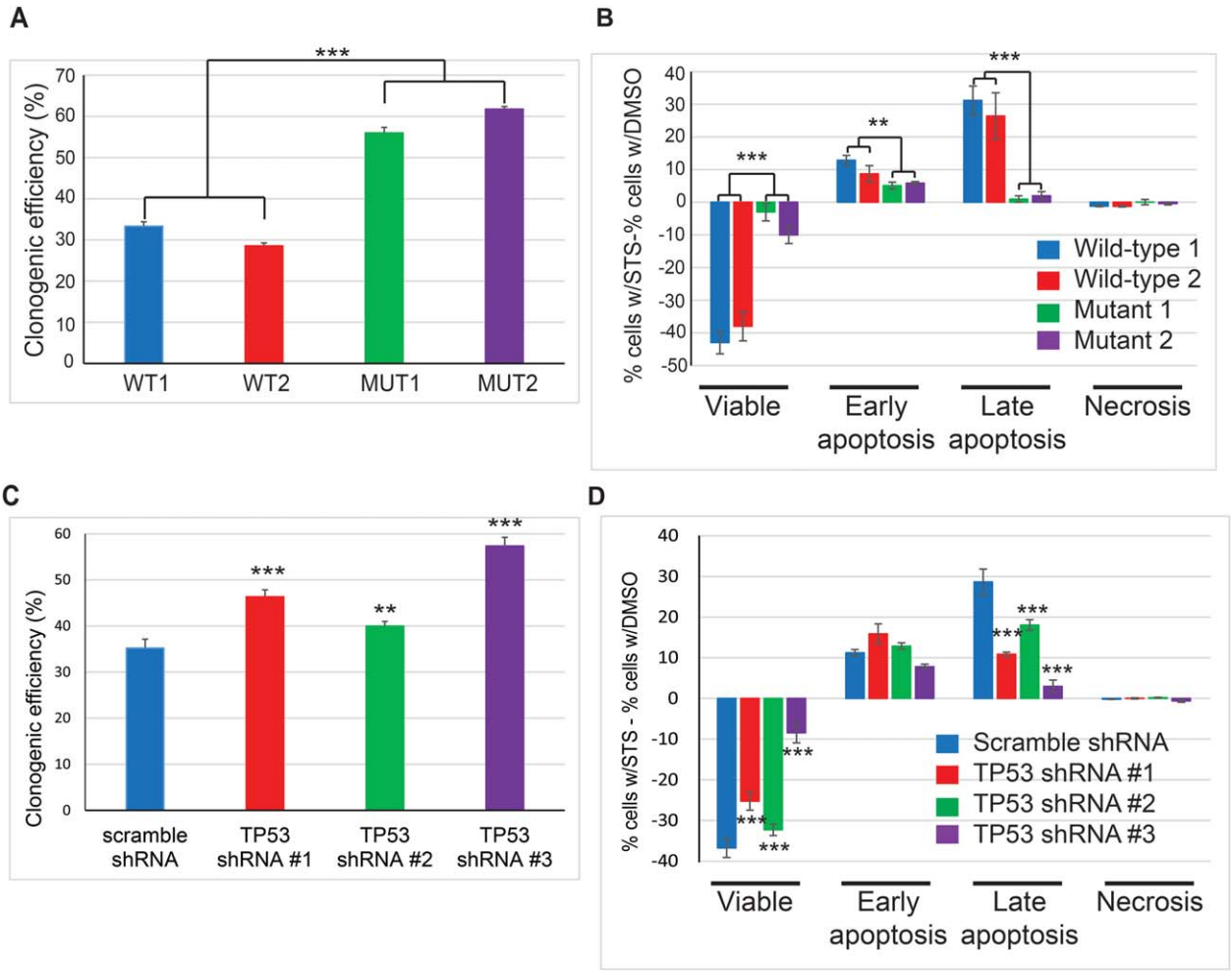

Figure 3. Clonogenicity and response to apoptotic stress of wild-type and mutant, and TP53 shRNA knockdown, hESC Clones. **(A, C)**: Clonogenic efficiency 7 days after low density plating (100 cells per well in 6 well plates) of mutant and wild-type cells (A) and scramble and TP53 shRNA clones made in wild-type clone 1 (C). See also Supporting Information Figure S4A, S4C. (B, **D**): Annexin V/PI staining and flow cytometry for quantification of apoptosis following 20 hours of 0.1 μM staurosporine treatment in wild-type and mutant clones (B) and scramble and TP53 shRNA clones made in wild-type clone 1 (D). For each category, the graph shows the difference between the percentages of cells with and without staurosporine treatment (the carrier, dimethyl sulfoxide (DMSO) was used as the negative control condition; the negative control without DMSO gave similar results as DMSO alone, data are not shown). See also Supporting Information Figure S4B, S4F. All data are expressed as the mean ± SEM of two or three independent biological experiments, and each experiment was conducted in triplicate. Statistical significance by two-tailed *t* test; $*p < .05$, $**p < .01$, $***p < .005$, wild-type versus mutant clones and scramble shRNA vs. *TP53* shRNA clones. Abbreviation: WT, wild type.

and late apoptosis, respectively) (Fig. 3B, Supporting Information Fig. S4B; Supporting Information Table S1).

Effect of Single-Copy Deletion of Chr17p13.1 on Repair of Etoposide-Induced DNA Damage in hESCs

The comet assay was used to evaluate DNA repair in response to the DNA damaging agent, etoposide. Cells were treated with etoposide overnight, and 24 hours after the etoposide was removed, the cell number, the average percent of DNA in the "tails" was calculated using OpenComet software package according to [39], and the percent of cells in each of five categories (Score 0 = no tail = no detectable DNA damage to Score 5 = longest tail = high degree of DNA damage) [40] was determined. We observed that the mutant clones displayed a markedly higher cell survival (Fig. 4A; Supporting Information Table S1), as well as evidence of significantly greater DNA damage by the comet assay, quantified both by the percentage of DNA in the tail (Fig. 4B; Supporting Information Table S1) and percent of cells with higher DNA damage scores (Fig. 4C; Supporting Information Table S1). These results suggest that cells with a single-copy deletion of chr17p13.1 may have not only an impaired DNA repair response, but also a higher tolerance for damaged DNA.

Effect of Single-Copy Deletion of Chr17p13.1 on Pluripotency and Differentiation Capacity of hESCs

We assessed the pluripotency of the wild-type and mutant clones by examining the expression of pluripotency markers and performing in vitro differentiation experiments. By immunocytochemistry, high expression of OCT4/POU5F1 and SSEA4 was observed in the undifferentiated state for all four clones (Supporting Information Fig. S5A, S5B). Likewise, RNA-Seq analysis showed that mRNA expression of OCT4/POU5F1, NANOG, SOX2, CD9, LIN28A, and LIN28B was high in all clones (Supporting Information Fig. S5C–S5H).

Differentiation capacity was determined using the EB and teratoma assays, demonstrating the ability of all four clones to differentiate toward all three germ layers (Fig. 5A, 5B, respectively). However, differences in EB morphology were observed. Whereas the wild-type EBs had a typical well-rounded morphology, the mutant EBs displayed irregular projections (Fig. 5C). In addition, the attachment efficiency of the mutant EBs was significantly lower than the wild-type EBs ($p = 3 \times 10^{-7}$) (Fig. 5D; Supporting Information Table S1). These findings are interesting because impairment of cell-cell and cell-matrix adhesion is characteristic of malignant cells and associated with dysfunction of TP53 [41]. Staining of plated EBs with an anti-OCT4 antibody showed that persistence of OCT4 protein expression was significantly higher for the wild-type versus mutant clones ($p = .00007$) (Fig. 5E;

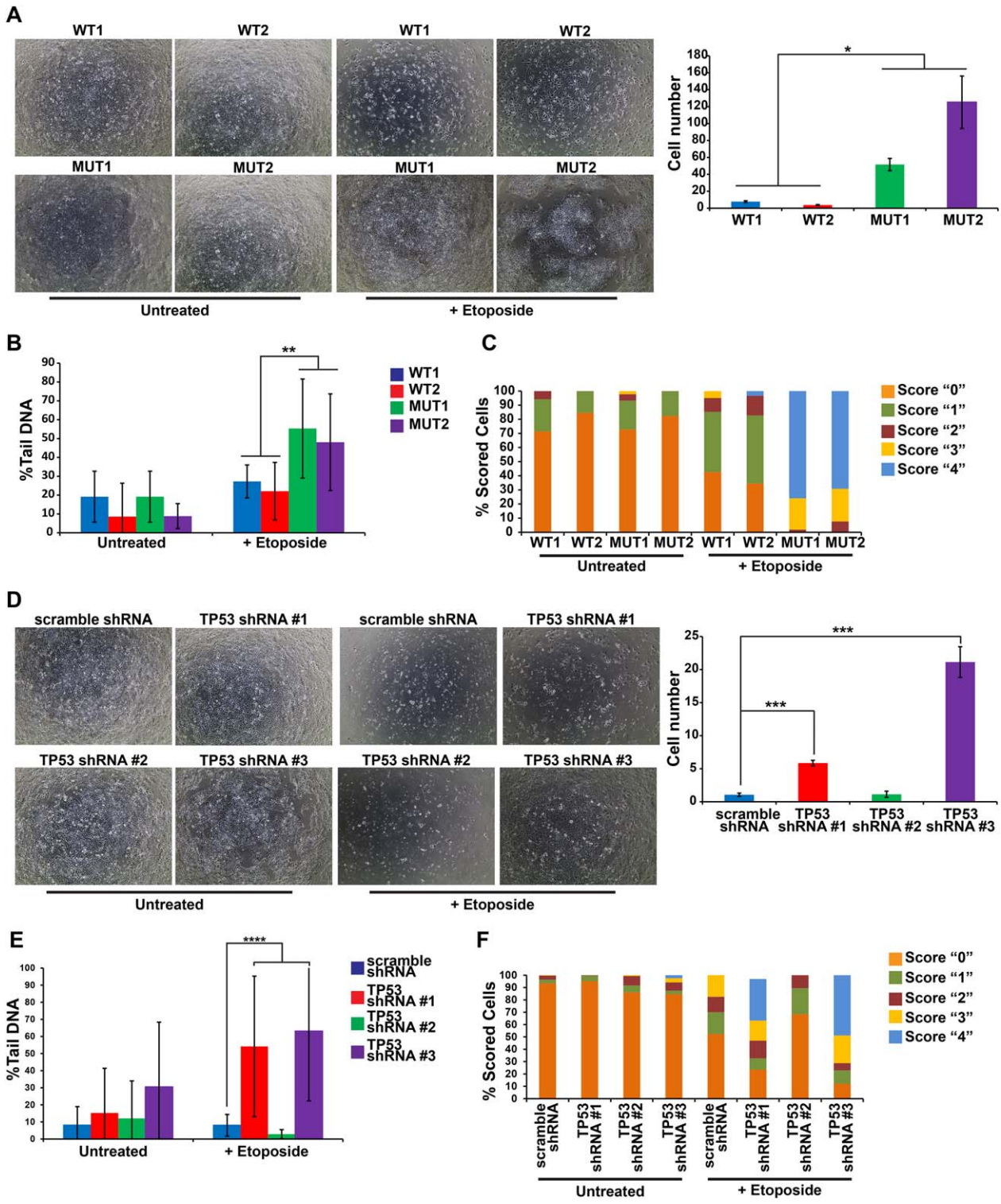

Figure 4.

Supporting Information Table S1). Residual OCT4-positive cells in differentiated cultures of hPSCs may represent a subpopulation of cells that are resistant to differentiation.

Effect of Single-Copy Deletion of chr17p13.1 on TP53 Expression

As mentioned above, we focused on the chr17p13.1 deletion in part because it encompassed the *TP53* gene. We previously showed that WA09 subcultures carrying single-copy loss of chr17p13.1 had decreased transcript expression of three genes in this genomic region: *TP53*, *SENP3*, and *SOX15* [5]. Given the known role of TP53 in regulation of cell survival and proliferation, we decided to focus on it as our initial target. First, we showed that the mutant clones have a 50% decrease in the basal protein expression level of TP53 compared to the wild-type clones ($p < .005$) (Fig. 6A; Supporting Information Table S1). TP53 plays a key role in the response of cells to stress conditions by inducing cell cycle arrest and apoptosis [17, 18], and both homozygous and single-copy loss-of-function of TP53 in cancer cells is correlated with increased cell proliferation, resistance to apoptotic stimuli, and poor prognosis. Therefore, we focused on the potential role of single-copy loss of *TP53* as a driver mutation conferring a selective advantage to our mutant clones. We tested this hypothesis by carrying out a battery of phenotypic assays aimed at quantifying parameters that reflect relevant cellular phenotypes.

Knockdown of *TP53* in hESCs Mimics the Majority of the Characteristics of the Chr17p13.1 Deletion Phenotype

To verify that the observed phenotypic differences between the wild-type and mutant clones were specifically caused by decreased expression of *TP53*, we performed knockdowns of *TP53* in the two wild-type clones.

Efficiency of shRNA-Mediated TP53 Knockdown in Wild-Type hESCs. We used a lentivirus-based shRNA system to stably knockdown TP53 expression in both wild-type clones, and investigated whether the resulting decreased expression of *TP53* recapitulates the mutant phenotype. Three independent shRNAs targeting TP53 (shRNA#1, shRNA#2, and shRNA#3) were transduced into wild-type cells. Relative expression of the *TP53* transcript in the resulting knockdown lines compared to a line transduced with a negative control shRNA (the "scramble" control) by qRT-PCR showed that all three shRNA constructs significantly decreased the expression of TP53 mRNA compared to the negative control shRNA (all p values $< 10^{-8}$). shRNA #3 had the strongest (95% knockdown), shRNA #2 the weakest (20%–40%) and shRNA #1 an intermediate effect (40%–60%) (Fig. 6B, Supporting Information Fig. S6A, S6B; Supporting Information Table S1). Protein expression mirrored the mRNA levels in the knockdown clones (Fig. 6C, Supporting Information Fig. S6C, S6D; Supporting Information Table S1). We note that based on TP53 protein levels, the shRNA #2 knockdown is likely to be most representative of the single-copy deletion of chr17p13.1 (Fig. 6C, 6D; Supporting Information Table S1).

Effect of TP53 Knockdown on Cell Proliferation. To examine whether TP53 knockdown confers a cell growth advantage on "minimal" E8 medium, as we observed for the chr17p13.1 deletion clones, we seeded the shRNA lines in MEF-CM and in E8 medium, and performed the MTT assay daily for four consecutive days. The proliferation rates of the knockdown clones were significantly higher than those of the scramble clone starting on day 3 in the cultures grown in E8 (Fig. 2C, 2D; Supporting Information Table S1). These results suggest that the loss of TP53 expression is responsible for more efficient cell proliferation in restrictive growth conditions seen in the chr17p13.1 deletion clones.

Effect of TP53 Knockdown on Clonogenic Potential. To determine whether targeted TP53 knockdown had a similar effect on colony formation as a single-copy deletion of chr17p13.1, we performed the clonogenic assay on the shRNA lines. All three TP53 shRNAs caused markedly increased colony formation compared to the negative control shRNA. Moreover, the increase in the number of colonies was correlated with the degree of TP53 knockdown (Fig. 3C, Supporting Information Fig. S4C, S4D; Supporting Information Table S1). These results indicated that TP53 plays an essential role in preventing survival and/or proliferation of hESCs in a single-cell context, as even partial inhibition of TP53 expression resulted in increased colony formation.

Effect of TP53 Knockdown on Staurosporine-Induced Apoptosis. To address whether TP53 mRNA knockdown mimics the decreased staurosporine-induced apoptosis in the mutant clones, we performed Annexin V/PI staining with FACS in the shRNA knockdown lines. After 20 hours of 0.1 μM staurosporine exposure, the wild-type clones transfected with any of the three TP53 shRNAs displayed significantly decreased late apoptosis compared with the negative control shRNA lines (all p values $< .007$, Fig. 3D, Supporting Information Fig. S4E–S4G; Supporting Information Table S1). The degree of reduction of sensitivity to staurosporine correlated with the efficiency of the *TP53* knockdown. These results indicated that TP53 is a

Figure 4. DNA repair in response to etoposide in wild-type and mutant, and TP53 shRNA knockdown, hESC clones. **(A–C)**: Effect of etoposide treatment on wild-type (WT1, WT2) and mutant (MUT1, MUT2) clones. **(D–F)**: Effect of etoposide treatment on scramble and knockdown TP53 hESC Clones. (A + D): Survival after Etoposide treatment (1 μM); in wild-type (WT1, WT2) and mutant (MUT1, MUT2) clones (A); in shRNA scramble and TP53 shRNA (#1, #2, #3) clones (D). On the left panel representative images from one of two replicate wells show cells density of wild-type and mutant clones (A) or of shRNA clones (D) in untreated and treated conditions. The right panel graph represents the average number of cells in the treated conditions. Data represent the average counts for three images per condition, with counts obtained for five fields per image. Asterisks indicate statistical significance by two-tailed t test; $*p < .001$, $***p < .0001$. (B + C), (E + F): Analysis of comet assay results for untreated and treated cells. (B + E): Graphs represent the percentage of damaged DNA present in the tail of cells treated or not treated with Etoposide. DNA damage was revealed by comet assay and analyzed using an open-source software package (see Methods). Asterisks indicate statistical significance by two-tailed t test; $**p < 10^{-11}$, $****p < 2 \times 10^{-5}$. (C + F): Stacked column graph indicates the percentage of nuclei scoring from 0 to 4 for each condition and clone. Scores range from 0, for nuclei showing intact DNA, to 4 for nuclei with a long come-like take, indicating highly damaged DNA. All phase-contrast images were taken at the same magnification (4×) using an EVOS imaging system.

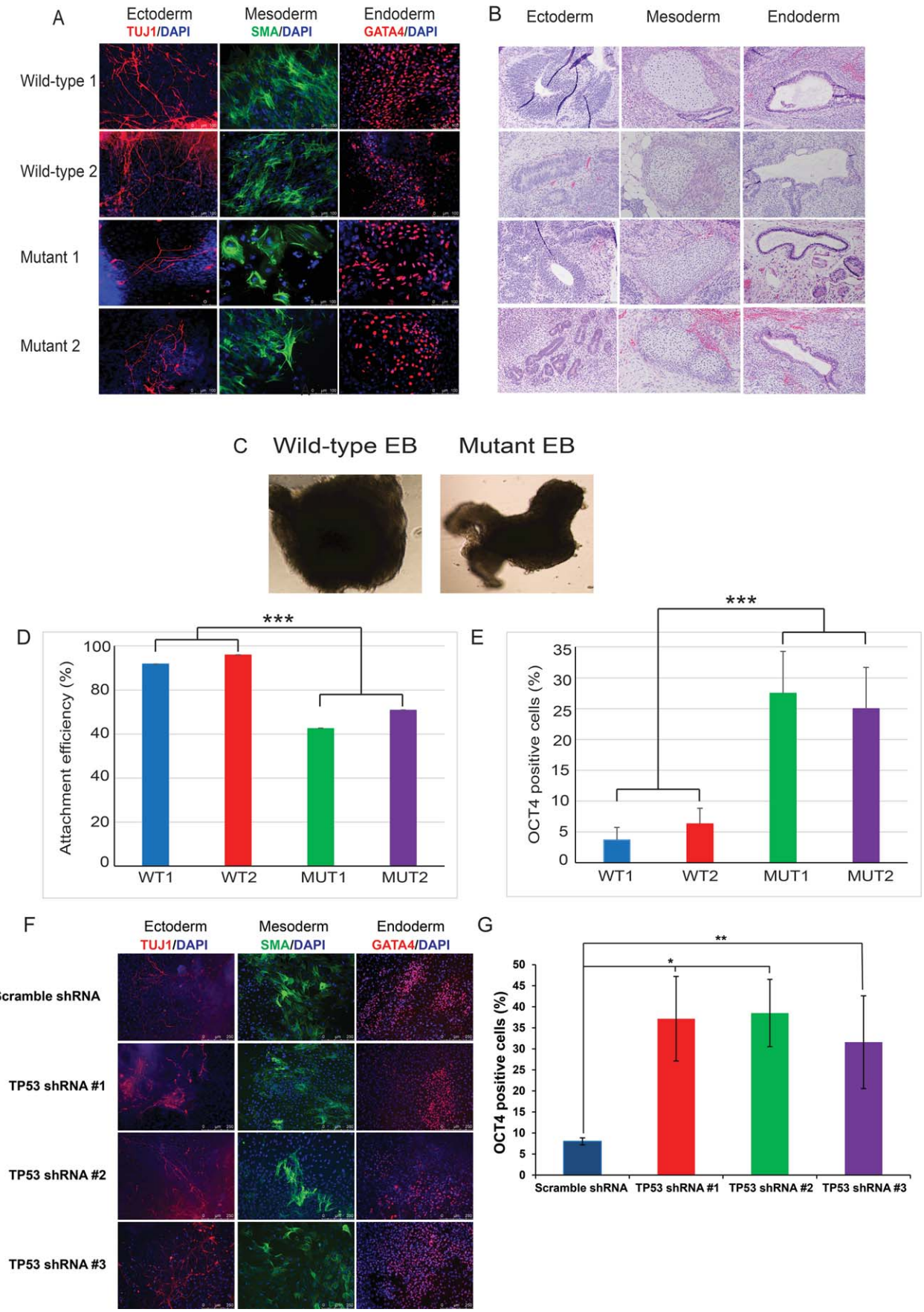

Figure 5.

mediator of apoptosis in hESCs treated with staurosporine, with the reduction of TP53 expression being protective against the staurosporine-induced apoptotic response in a dose dependent manner.

Effect of TP53 Knockdown on Repair of Etoposide-Induced DNA Damage in hESCs. DNA repair in response to the DNA damaging agent, etoposide, was again assessed using the comet assay. Cells were treated with etoposide overnight, and assessed 24 hours after the etoposide was removed. Compared to the scramble shRNA control clone, the TP53 shRNA knockdown clones displayed markedly higher cell survival (Fig. 4D; Supporting Information Table S1), as well as evidence of significantly greater DNA damage by the comet assay, quantified both by the percentage of DNA in the tail (Fig. 4E; Supporting Information Table S1) and percent of cells with higher DNA damage scores (Fig. 4F; Supporting Information Table S1). These results support the hypothesis that decreased expression of TP53 in the chr17p13.1 mutant cells is responsible for the impaired DNA damage response and greater survival in the presence of DNA damage observed above.

Effect of TP53 Knockdown on Differentiation of hESCs. Similar to both the wild-type and mutant clones, scramble and TP53 knockdown hESCs were all able to differentiate to all three germ lineages using the EB assay (Fig. 5F). Moreover, the TP53 shRNA knockdown clones all displayed a higher percentage of OCT4-positive cells after 2 weeks of differentiation in the EB assay (Fig. 5G; Supporting Information Table S1). One difference between the TP53 knockdown clones and the chr17p13.1 deletion mutant clones, was that the knockdown clones did not display decreased expression of early lineage-specific genes compared to the scramble shRNA control (Supporting Information Fig. S2E; Supporting Information Table S1). This suggests that TP53 may contribute to the regulation pluripotency genes, such as *OCT4/POU5F1*, but may not be required for cellular differentiation. In addition, it is possible that one of the other genes encompassed in the chr17p13.1 deletion may be contributing to the decreased expression of early lineage-specific genes in the mutant clones.

Discussion

There is ample evidence that hPSCs acquire genomic aberrations in culture. These include both "common," or recurrent, mutations that have been found many times in multiple hPSC lines, such as duplications of chr12p13.31 and chr20q11.21 [3, 7–10], and "sporadic" aberrations, which as a group observed frequently in hPSC cultures, but which individually have not been reported repetitively [5, 42]. One of the common genetic alterations, duplication of chr20q11.21, has been reported to confer a selective advantage to hPSCs in culture [15, 16]. However, no studies have examined the phenotypic significance of sporadic genomic aberrations in hPSC cultures.

In this study, we focused on one such sporadic genomic aberration. Specifically, we identified novel single-copy losses of portions of chromosome 17, all of them encompassing chr17p13.1, in several subcultures of the WA09 hESC line [5]. Homozygous loss of this genomic region is strongly associated with cancer, but there is growing evidence that single-copy loss is associated with refractory disease [19–22, 43]. Therefore, we hypothesized that this single-copy deletion might affect the behavior of our cells, and set out to characterize the phenotypes of hESCs with and without this mutation. Since this region of the genome contains the known tumor-suppressor gene, *TP53*, we also asked whether the specific single-copy loss of *TP53* was a key driver of the observed phenotypic changes.

To identify phenotypes on which to focus, we performed RNA-Seq on the wild-type and chr17p13.1 deletion mutant clones, and our differential expression and pathway analysis results pointed to increased cell proliferation, decreased biological adhesion, decreased apoptosis, decreased DNA repair, and decreased cell differentiation in the mutant clones. Accordingly, we evaluated cell proliferation, clonogenicity, response to apoptotic stress, capacity for DNA repair, and differentiation capacity of the clones.

Our results showed that mutant clones containing a single-copy deletion of chr17p13.1 exhibited significantly increased proliferation when cultured in defined medium, a decreased rate of cell death (but increased DNA damage seen in surviving cells) with DNA damage induced by etoposide, enhanced clonogenic efficiency after low density plating, and decreased levels of apoptosis upon staurosporine treatment. These data support the conclusion that this deletion confers a selective advantage to hESCs when exposed to specific stresses, including culture in minimal media conditions (represented by E8 medium), DNA damage, low cell density, and apoptotic stress.

In the cancer literature, single-copy deletions encompassing chr17p13.1 are strongly correlated with high-risk disease, including inferior response to standard treatments, recurrent disease and shorter survival in chronic lymphocytic leukemia [20, 21], non-Hodgkin lymphomas [19], multiple myeloma [22], and pediatric medulloblastoma [43]. The *TP53* gene is located in this genomic region, and mutations in *TP53* have been associated with higher tumorigenicity and resistance to drug-induced apoptosis in a variety of tumor cells [17, 18], and loss

Figure 5. Differentiation potential of wild-type and mutant, and TP53 shRNA knockdown, hESC clones. **(A + F)**: In vitro differentiation of the wild-type and mutant (A) and TP53 shRNA knockdown (F) clones was shown by EB formation. The EBs were stained with 2-(4-amidinophenyl)-1H-indole-6-carboxamidine (DAPI) and the tissue-specific markers TUJ1 for ectoderm, smooth muscle actin (SMA) for mesoderm, and GATA4 for endoderm. Representative images are shown (scale bar 100 μm). **(B)**: In vivo differentiation of wild-type and mutant clones demonstrated by teratoma formation. The tissues from the teratomas were identified using hemotoxylin and eosin staining. Representative images are shown (scale bar 100 μm). **(C)**: Morphology of EBs formed from wild-type (left) and mutant (right) clones after 7 days. **(D)**: Attachment efficiency of EBs on gelatin-coated coverslips. Attachment assay: 24 replicates per clone were performed, with each replicate consisting of three EBs seeded into one well. **(E + G)**: Expression of the pluripotency marker OCT4/POU5F1 after 2 weeks of EB differentiation for wild-type and mutant (E) and TP53 shRNA mutant (G) clones. OCT4 expression assay: three coverslips were generated per clone, with three EBs seeded per coverslip; five high-power fields per coverslip were used for quantification, and the quantification was performed twice by two different examiners in a blinded fashion. All data are expressed as the mean ± SEM, asterisks indicate statistical significance by two-tailed *t* test; *$p < .05$, **$p < .01$, ***$p < .005$, wild-type versus mutant clones and scramble shRNA vs. *TP53* shRNA clones. Abbreviation: EB, embryoid body; MUT, mutant; WT, wild type.

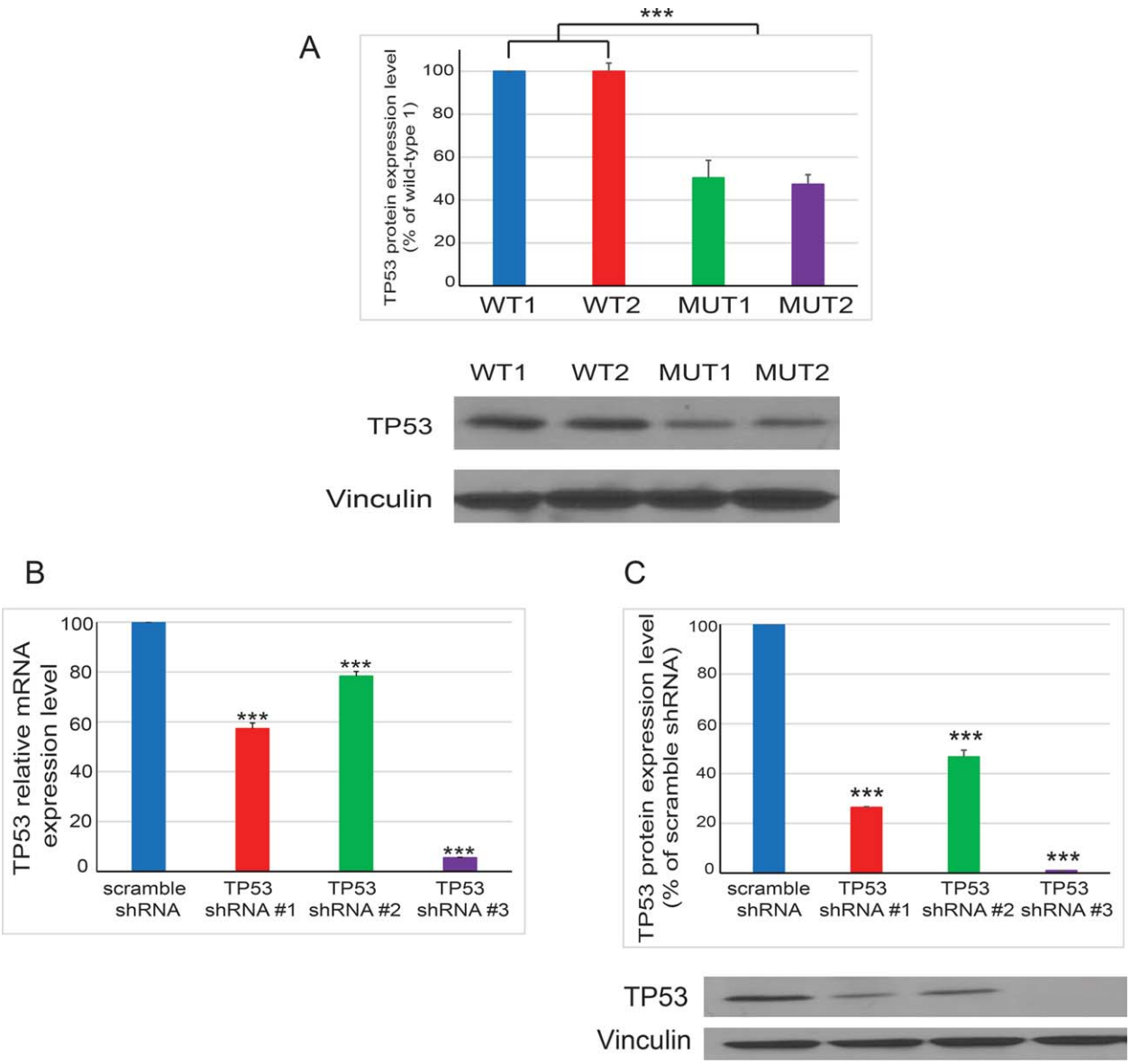

Figure 6. Knockdown of *TP53* in wild-type clone 2 (WT2). **(A)**: Quantitative analysis of TP53 protein levels in the wild-type and the mutant cells. Data are expressed as the mean ± SEM of three independent biological samples. Wild-type clone 1 was used as reference. A representative western blot for TP53 is shown below the graph. Vinculin was used as a loading control. **(B)**: Relative mRNA expression of *TP53* transcript in WT2 with three different *TP53* knockdown shRNAs compared to the negative control (scramble) shRNA. Data are expressed as the mean ± SEM of two independent biological experiments, with each experiment including 3–5 technical replicates. See also Supporting Information Figure S6A, S6B. **(C)**: Quantitative analysis of TP53 protein levels in the WT2 with the three different *TP53* knockdown shRNAs compared to the negative control shRNA. Data are expressed as the mean ± SEM of three independent biological samples. A representative western blot for TP53 is shown below the graph. Vinculin was used as a loading control. See also Supporting Information Figure S6C, S6D. ***$p < .000001$. Abbreviation: MUT, mutant; WT, wild type.

of *TP53* is thought to be the primary driver of poor outcomes in cancers containing single-copy deletions of chr17p13.1 [19–22, 43]. In mESCs and hESCs, TP53 has been shown to play an important role in regulation of cell proliferation, cell cycle progression, apoptosis and differentiation [27, 28, 30, 44–47]. Consistent with these previous reports, we were able to recapitulate the selective advantage of the mutant clones in the cell proliferation, DNA damage, clonogenicity, and apoptosis assays, by knocking down *TP53* expression in the wild-type clones using shRNA constructs, thus supporting the conclusion that loss of TP53 is the primary factor conferring a survival advantage to the mutant clones in our system.

We found that the wild-type and mutant clones and the shRNA clones expressed high levels of pluripotency markers, including *NANOG* and *OCT4*, in the undifferentiated state, and also efficiently differentiated into cell types representing all three germ layers. However, we observed persistent OCT4 expression in many more cells in the mutant and TP53 shRNA EBs in comparison with the wild-type and scramble shRNA EBs, respectively. Moreover, we observed that while the wild-type clones formed typical smoothly rounded EBs, the mutant clones formed complex EBs with irregular projections and also did not attach to the tissue culture plate as efficiently as wild-type clones. Interestingly, this unusual EB morphology and poor

attachment was not seen in the TP53 shRNA knockdown clones (data not shown). This partial discordance in behavior in the differentiation assays between the mutant and TP53 shRNA knockdown clones suggests that the loss of TP53 is not responsible for all of the differentiation phenotypes seen in the chr17p13.1 deletion mutants, and that other genes encompassed in the deleted region may also contribute to the phenotype. This possibility is also supported by the observation that, in the undifferentiated state, the mutant clones expressed lower levels of transcription factors associated early lineage commitment compared to the wild-type clones, while the TP53 shRNA knockdown clones expressed similar or higher levels of these transcripts than the scramble shRNA control clone.

We note that in addition to the single-copy deletion of chr17p13.1 in the mutant clones, the mutant and wild-type clones were discordant for genetic aberrations at other genomic locations. In this study, we focused on the chr17p13.1 region, given the fact the *TP53* gene is located within it. Our results comparing the mutant and wild-type clones, along with the TP53 shRNA knockdowns, indicate that the single-copy chr17p13.1 is at least partially responsible for the difference in phenotype between the mutant and wild-type clones. We recognize that the other aberrations may also contribute to the phenotypic differences between the mutant and wild-type clones. The difference in CN for the chr20q11.21 region (three copies in the mutant clones and five copies in the wild-type clones) should have conferred an advantage to the wild-type clones, and thus our results suggest that the single-copy chr17p13.1 deletion in the mutant clones may have a stronger effect than the additional two copies of the chr20q11.21 region in the wild-type clones. The other discordant aberrations have not been previously studied in detail in hESCs and should be investigated in future studies. However, we would like to point out the potential concerns related to discordant aberrations at other genomic loci do not apply to the shRNA experiments, as the TP53 knockdown and control clones were isogenically matched. Moreover, these knockdowns were performed in both of the "wild-type" clones, with concordant results.

It is possible that the likelihood of a deletion of the chr17p13.1 region is increased by a prior duplication of chr12p, which has been linked to genetic instability [14]. However, in our prior study, there were subcultures of hESCs that contained the chr17p13.1 deletion without a duplication of chr12p [5], indicating that the occurrence of the chr17p13.1 deletion is not predicated on a chr12p duplication.

Conclusion

To our knowledge, this is the first study to report the phenotype of a sporadic spontaneous mutation in hESCs. We have shown that this mutation, a single-copy deletion of chr17p13.1, has important effects on hESC proliferation and survival, and that the loss of one copy of the *TP53* gene is likely to be the key driver mutation. Moreover, we observed that this mutation resulted in aberrant persistence of OCT4 expression after spontaneous differentiation. Our findings suggest that human pluripotent stem cell cultures intended for preclinical or clinical use should be tested not only for common genomic aberrations, but also for sporadic aberrations. We recognize that it will be challenging to determine the phenotypic consequences, particularly the tumorigenicity, of each observed sporadic aberration, and that novel experimental and bioinformatics approaches to this problem will need to be developed.

Acknowledgments

The research was funded by the UCSD Department of Reproductive Medicine and the California Institute of Regenerative Medicine (TR3-05603 to L.C.L. and J.F.L., CL1-00502 and TR1-01250 to J.F.L., and postdoctoral scholar award to I.G.). K.S. was supported by an unrestricted award from Millipore, Inc. We thank Francesca S. Boscolo and Trevor R. Leonardo for the assistance with the CNV analysis, Marwa Khater for the assistance with the analysis of RNA-Seq data, and Mana Parast and Ying-Chun Li for histopathologic analysis of the teratomas. Thanks to Dwayne Stupack for critical reading of the manuscript. The authors declare no conflict of interest. K.S. is currently affiliated with Stanford School of Medicine, Pasca Lab; Department of Psychiatry and Behavioral Sciences, Center for Sleep Sciences and Medicine, Palo Alto, CA; I.G. is currently affiliated with International Stem Cell Corporation, Carlsbad, CA.

Author Contributions

A.H.: conception and design, collection and/or assembly of data, data analysis and interpretation, manuscript writing, final approval of manuscript; T.T., K.S.: collection and/or assembly of data, final approval of manuscript; D.C.: data analysis and interpretation, final approval of manuscript; I.G.: contribution of resources, final approval of manuscript; J.F.L.: contribution of resources, financial support, final approval of manuscript; R.M.: data analysis and interpretation, final approval of manuscript; L.C.L.: conception and design, financial support, collection and/or assembly of data, data analysis and interpretation, manuscript writing, final approval of manuscript.

Disclosure of Potential Conflicts of Interest

The authors indicate no potential conflicts of interest.

Accession Numbers

The GEO accession numbers: GSE70874 (RNA-Seq), GSE70828 (SNP), GSE70875 (SuperSeries).

References

1 Maitra A, Arking DE, Shivapurkar N et al. Genomic alterations in cultured human embryonic stem cells. Nat Genet 2005;37:1099–1103.

2 Lund RJ, Narva E, Lahesmaa R. Genetic and epigenetic stability of human pluripotent stem cells. Nat Rev Genet 2012;13:732–744.

3 Laurent LC, Ulitsky I, Slavin I et al. Dynamic changes in the copy number of pluripotency and cell proliferation genes in human ESCs and iPSCs during reprogramming and time in culture. Cell Stem Cell 2011;8:106–118.

4 Bai Q, Ramirez JM, Becker F et al. Temporal analysis of genome alterations induced by single-cell passaging in human embryonic stem cells. Stem Cells Dev 2015;24:653–662.

5 Garitaonandia I, Amir H, Boscolo FS et al. Increased risk of genetic and epigenetic instability in human embryonic stem cells associated with specific culture conditions. PLoS One 2015;10:e0118307.
6 Catalina P, Montes R, Ligero G et al. Human ESCs predisposition to karyotypic instability: Is a matter of culture adaptation or differential vulnerability among hESC lines due to inherent properties? Mol Cancer 2008;7:76.
7 Baker DE, Harrison NJ, Maltby E et al. Adaptation to culture of human embryonic stem cells and oncogenesis in vivo. Nat Biotechnol 2007;25:207–215.
8 Draper JS, Smith K, Gokhale P et al. Recurrent gain of chromosomes 17q and 12 in cultured human embryonic stem cells. Nat Biotechnol 2004;22:53–54.
9 Amps K, Andrews PW, Anyfantis G et al. Screening ethnically diverse human embryonic stem cells identifies a chromosome 20 minimal amplicon conferring growth advantage. Nat Biotechnol 2011;29:1132–1144.
10 Lefort N, Feyeux M, Bas C et al. Human embryonic stem cells reveal recurrent genomic instability at 20q11.21. Nat Biotechnol 2008;26:1364–1366.
11 Spits C, Mateizel I, Geens M et al. Recurrent chromosomal abnormalities in human embryonic stem cells. Nat Biotechnol 2008;26:1361–1363.
12 Mostert M, Rosenberg C, Stoop H et al. Comparative genomic and in situ hybridization of germ cell tumors of the infantile testis. Lab Invest 2000;80:1055–1064.
13 Rodriguez E, Houldsworth J, Reuter VE et al. Molecular cytogenetic analysis of i(12p)-negative human male germ cell tumors. Genes Chromosomes Cancer 1993;8: 230–236.
14 Moon SH, Kim JS, Park SJ et al. Effect of chromosome instability on the maintenance and differentiation of human embryonic stem cells in vitro and in vivo. Stem Cell Res 2011;6:50–59.
15 Avery S, Hirst AJ, Baker D et al. BCL-XL mediates the strong selective advantage of a 20q11.21 amplification commonly found in human embryonic stem cell cultures. Stem Cell Rep 2013;1:379–386.
16 Nguyen HT, Geens M, Mertzanidou A et al. Gain of 20q11.21 in human embryonic stem cells improves cell survival by increased expression of Bcl-xL. Mol Hum Reprod 2014; 20:168–177.
17 Levine AJ, Oren M. The first 30 years of p53: Growing ever more complex. Nat Rev Cancer 2009;9:749–758.
18 Brosh R, Rotter V. When mutants gain new powers: News from the mutant p53 field. Nat Rev Cancer 2009;9:701–713.
19 Halldorsdottir AM, Lundin A, Murray F et al. Impact of TP53 mutation and 17p deletion in mantle cell lymphoma. Leukemia 2011;25:1904–1908.
20 Puiggros A, Blanco G, Espinet B. Genetic abnormalities in chronic lymphocytic leukemia: Where we are and where we go. BioMed Res Int 2014;2014:435983.
21 Shindiapina P, Brown JR, Danilov AV. A new hope: Novel therapeutic approaches to treatment of chronic lymphocytic leukaemia with defects in TP53. Br J Haematol 2014; 167:149–161.
22 Teoh PJ, Chung TH, Sebastian S et al. p53 haploinsufficiency and functional abnormalities in multiple myeloma. Leukemia 2014;28:2066–2074.
23 Gonzalez D, Martinez P, Wade R et al. Mutational status of the TP53 gene as a predictor of response and survival in patients with chronic lymphocytic leukemia: Results from the LRF CLL4 trial. J Clin Oncol 2011;29: 2223–2229.
24 Jain N, O'brien S. Chronic lymphocytic leukemia with deletion 17p: Emerging treatment options. Oncology (Williston Park) 2012;26:1067, 1070.
25 Rossi D, Khiabanian H, Spina V et al. Clinical impact of small TP53 mutated subclones in chronic lymphocytic leukemia. Blood 2014;123:2139–2147.
26 Solozobova V, Blattner C. p53 in stem cells. World J Biol Chem 2011;2:202–214.
27 Sabapathy K, Klemm M, Jaenisch R et al. Regulation of ES cell differentiation by functional and conformational modulation of p53. EMBO J 1997;16:6217–6229.
28 Qin H, Yu T, Qing T et al. Regulation of apoptosis and differentiation by p53 in human embryonic stem cells. J Biol Chem 2007;282:5842–5852.
29 Solozobova V, Rolletschek A, Blattner C. Nuclear accumulation and activation of p53 in embryonic stem cells after DNA damage. BMC Cell Biol 2009;10:46.
30 Grandela C, Pera MF, Grimmond SM et al. p53 is required for etoposide-induced apoptosis of human embryonic stem cells. Stem Cell Res 2007;1:116–128.
31 Fan T, Tian F, Yi S et al. Implications of Bit1 and AIF overexpressions in esophageal squamous cell carcinoma. Tumour Biol 2014; 35:519–527.
32 Hua W, Miao S, Zou W et al. Pathological implication and function of Bcl2-inhibitor of transcription in ovarian serous papillary adenocarcinomas. Neoplasma 2013;60:143–150.
33 Jan Y, Matter M, Pai JT et al. A mitochondrial protein, Bit1, mediates apoptosis regulated by integrins and Groucho/TLE corepressors. Cell 2004;116:751–762.
34 Richardson AL, Wang ZC, De Nicolo A et al. X chromosomal abnormalities in basal-like human breast cancer. Cancer Cell 2006;9: 121–132.
35 Younes A, Jendiroba D, Katz R et al. Chromosome X numerical abnormalities in patients with non-Hodgkin's lymphoma. A study of 59 patients using fluorescence in situ hybridization. Cancer Genet Cytogenet 1995;82:23–29.
36 Fernandez-Jimenez N, Castellanos-Rubio A, Plaza-Izurieta L et al. Accuracy in copy number calling by qPCR and PRT: A matter of DNA. PloS One 2011;6:e28910.
37 Kurosawa H. Application of Rho-associated protein kinase (ROCK) inhibitor to human pluripotent stem cells. J Biosci Bioeng 2012;114:577–581.
38 Chappell WH, Lehmann BD, Terrian DM et al. p53 expression controls prostate cancer sensitivity to chemotherapy and the MDM2 inhibitor Nutlin-3. Cell Cycle 2012; 11:4579–4588.
39 Gyori BM, Venkatachalam G, Thiagarajan PS et al. OpenComet: An automated tool for comet assay image analysis. Redox Biol 2014; 2:457–465.
40 Collins AR. The comet assay for DNA damage and repair: Principles, applications, and limitations. Mol Biotechnol 2004;26:249–261.
41 Rivlin N, Brosh R, Oren M et al. Mutations in the p53 tumor suppressor gene: Important milestones at the various steps of tumorigenesis. Genes Cancer 2011;2:466–474.
42 Narva E, Autio R, Rahkonen N et al. High-resolution DNA analysis of human embryonic stem cell lines reveals culture-induced copy number changes and loss of heterozygosity. Nat Biotechnol 2010;28:371–377.
43 Park AK, Lee SJ, Phi JH et al. Prognostic classification of pediatric medulloblastoma based on chromosome 17p loss, expression of MYCC and MYCN, and Wnt pathway activation. Neuro Oncol 2012;14:203–214.
44 Corbet SW, Clarke AR, Gledhill S et al. P53-dependent and -independent links between DNA-damage, apoptosis and mutation frequency in ES cells. Oncogene 1999; 18:1537–1544.
45 Lee MK, Hande MP, Sabapathy K. Ectopic mTERT expression in mouse embryonic stem cells does not affect differentiation but confers resistance to differentiation- and stress-induced p53-dependent apoptosis. J Cell Sci 2005;118:819–829.
46 Lin T, Chao C, Saito S et al. p53 induces differentiation of mouse embryonic stem cells by suppressing Nanog expression. Nat Cell Biol 2005;7:165–171.
47 Maimets T, Neganova I, Armstrong L et al. Activation of p53 by nutlin leads to rapid differentiation of human embryonic stem cells. Oncogene 2008;27:5277–5287.
48 Kanehisa M, Goto S, Sato Y et al. Data, information, knowledge and principle: Back to metabolism in KEGG. Nucleic Acids Res 2014;42:D199–D205.

See www.StemCells.com for supporting information available online.